Asian Journal of Chemistry; Vol. 25, No. 3 (2013), 1259-1264

ASIAN JOURNAL OF CHEMISTRY

http://dx.doi.org/10.14233/ajchem.2013.12817

Homology Modeling and Molecular Dynamics Study of C-Terminal Catalytic Domain of Human Protein Kinase D1

YONG SHAN ZHAO[1,*], YANG XU[1], KUN WANG[1], HONG ZENG[1], JIAN WANG[2], SHENG CHENG MAO[2] and JING HAI ZHANG[1]

[1]School of Life Science and Bio-Pharmaceutics, Shenyang Pharmaceutical University, Shenyang 110016, Liaoning Province, P.R. China
[2]School of Pharmaceutical Engineering, Shenyang Pharmaceutical University, Shenyang, P.R. China

*Corresponding author: Tel/Fax: +86 24 23986399; E-mail: zhao09081@yahoo.cn

(*Received*: 5 October 2011; *Accepted*: 7 September 2012) AJC-12093

The three-dimensional (3D) model of the C-terminal catalytic domain of human protein kinase D1 (hPKD1c) was constructed based on the crystal structure of the protein kinase Chk2 (PDB code 2CN5) in complex with ADP using Modeller9v2 program. With the aid of molecular mechanics and molecular dynamics method, the last model was obtained and further assessed by Procheck, Prosa2003 and Profile-3D, which confirms that the refined model is reliable. Furthermore, the docking results of Gö6976 1 and its structural analogues into the active site of hPKD1c indicate that 2,6-naphthyridine 13c is a more preferred ligand than others, which is in good agreement with the experimental results. From the docking studies, we also suggest that Ser12, Lys82, Leu83, His84, Asp86, Glu89 and Leu134 in the hPKD1c are important determinant residues in binding as they have strong electrostatic interactions with the ligand.

Key Words: Protein kinase D, Docking, Homology modeling.

INTRODUCTION

Human protein kinase D1 (hPKD1)[1] belongs to the serine/threonine kinase family, which has emerged as a key regulator of many important cellular processes, including proliferation, differentiation, migration and death[2,3]. Recent studies of hPKD1 inactivation suggest that this enzyme could be an attractive target for the treatment of heart failure[4,5], tumor[6] or cancer[7-9].

Despite the therapeutic potential of hPKD1 in various diseases, only a few potent and selective inhibitors have been identified. Until recently, the ATP-competitive inhibitors of hPKD1 with greatly improved selectivity have been described. However, no report has been found about the three-dimensional (3D) structure of hPKD1, which has seriously hampered further determination of biological roles and structure-based design of potent and selective inhibitors of hPKD1. Thus, knowledge of the 3D structure is essential for understanding the relationship of enzyme function and structure and theoretical studies on the binding mode of the hPKD1 with its inhibitors are necessary to reveal the interaction occurring in the active site.

To our best of knowledge, the homology modeling is an efficient method for the 3D structure construction of proteins[10-12]. In this paper, we first tried to obtain a reliable 3D structure of the C-terminal catalytic domain of the hPKD1 (hPKD1c) based on protein kinase Chk2 (PDB code 2CN5) by the homology modeling method, followed by molecular mechanics (MM) and molecular dynamics (MD) simulation to refine the initial model. The quality of the resulting substrate-free 3D model of hPKD1c was critically assessed *via* geometric and energetic assessments. Subsequently, the model structure was used to search the active site and carried out binding studies by flexible docking with Gö6976 **1** and its structural analogues. Finally, according to the analysis, in the docked complexes, certain key residues responsible for the substrate specificity were identified. The results might be a good starting point for further determination of the biological role and structure based inhibitor design of the hPKD1.

EXPERIMENTAL

Homology modeling: The primary sequence of hPKD1c (Accession No. Q15139) was obtained from the SWISS-PROT and TrEMBL database of the ExPASy Molecular Biology Server[13]. The first step was searching a number of related sequences to find a related protein as a template by the BLAST program[14] (http://www.ncbi.nih.gov) and then the sequence alignment was performed by ClustalW program[15] (version 1.83) using a gap penalty of 10 and employing BLOSUM30 weight matrix. Program Modeler9v2[16] is performed to build the 3D structure of hPKD1c. Modeler is an implementation of an automated approach to comparative modeling by satisfaction

of spatial restraints[17,18]. Within Modeler, the sequence alignment is used to generate several models and the outcomes were ranked on the basis of the internal scoring function of the program. The model with the highest score was validated by probability density functions and chosen for further refinement.

Molecular dynamics simulation: The tleap module in Amber10[19] was used to generate an all-atom model of hPKD1c on the basis of the initial model and then the protein was solvated in a rectangular box of explicit boundary solvent water molecules to account for solvent effects. The TIP3P model[20] was used and the water box extended 9 Å away from any solute atom.

Prior to molecular dynamics simulations, a series of minimizations were performed. All water molecules were first minimized while restraining the protein atomic positions with a harmonic potential. The system was then energy-minimized without restraints for 2000 steps using a combination of steepest descent and conjugated gradient methods. After the system was gradually heated from 10 to 300 K over 20 ps using the NVT ensemble, the molecular dynamics simulation is carried out to examine the quality of the model structures by checking their stability *via* performing 1ns simulation at 1 atm and 300 k with the NPT ensemble. During the simulation, SHAKE algorithm[21] was applied to constrain the covalent bonds to hydrogen atoms. A time step of 2 fs and a nonbond interaction cutoff radius of 10 Å were used. Coordinates were saved every 5ps during the entire process. The ff03 all atom Amber force field[22] was used for the protein.

The lowest energy structure during 1ns simulation was calculated. After removing the water molecules, the lowest energy structure was submitted for energy minimization with a conjugate gradient method for 3000 steps. In this step, the quality of the initial model is improved.

After the optimization procedure, the final 3D model of hPKD1c was checked using Profile-3D[23], Procheck[24] and Prosa2003[25]. The Profile-3D method measured the compatibility of an amino acid sequence with a known 3D protein structure. Procheck was employed for geometric evaluations and Prosa2003 was used to evaluate the quality of consistency between the native fold and the sequence and to examine the energy of residue-residue interactions.

Docking inhibitors to hPKD1c: The initial structures of Gö6976 1 and its structural analogues were built and minimized using CHARMm force field, until a convergence gradient of 0.02 kcal/mol was accomplished. The two-dimensional structures of all of these inhibitors are shown in Fig. 1. The docking studies[26] were performed by the flexible docking module in DS 2.5. A key feature is that the "bulk" of the receptor, defined as atoms which are not in the binding site specified, is held rigid during the docking process, while the binding site atoms and ligand atoms are movable. To account the solvent effect, the centered enzyme-ligand complex was solvated in layers of TIP3P water molecules with 9 Å. Finally, the docked complex of hPKD1c with Gö6976 1 and its structural analogues were selected by the criteria of interacting energy combined with the geometrical matching quality. The complex was used as the staring conformation for further energetic minimization and geometrical optimization before the final model was

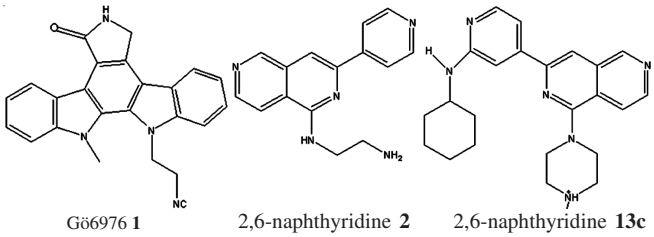

Gö6976 **1** 2,6-naphthyridine **2** 2,6-naphthyridine **13c**

Fig. 1. Structure of Gö6976 **1**, 2,6-naphthyridine **2** and 2,6-naphthyridine **13c**

generated. The global structure with the lowest energy was chosen for computing intermolecular binding energies.

RESULTS AND DISCUSSION

A high level of sequence identity should guarantee more accurate alignment between the target sequence and template structure. In the result of the BLAST search, the high sequence identity between the hPKD1 and 2CN5 is 39 % which allows for rather straightforward sequence alignment (Fig. 2). Automated homology model building was performed using protein structure modeling program Mod eler9v2. The best ranked model was chosen based on probability density functions. With this procedure, the initial model was complete. This model was refined by molecular mechanics optimization and molecular dynamics simulations and then the final stable structure of hPKD1c was obtained as displayed in Fig. 3a. From Fig. 3a, we can see that this enzyme has 11 helices and 8 sheets.

The conformation with the lowest energy was chosen and the 3D structure was superimposed with 2CN5. Their root mean square deviation (RMSD) value is 1.38 Å (Fig. 3b), indicating a good overall structure alignment with 2CN5. The final structure with the lowest energy was checked by profile-3D and the self-compatibility score for this protein is 96.28, which is higher than the low score 53.80 and closed to the top score 119.55. And then, the structure of hPKD1c was evaluated using Procheck and Prosa2003. The statistical score of the Rmamchandran plot shows that 88.3 % are in the most favoured regions, 9.5 % in the additional allowed regions and 2.2 % in generously allowed regions. The z-score and overall score of Procheck geometric assessment are -7.16 and -0.07, respectively. The above results indicate that the homology model is reliable.

Fig. 4(a,b) display the total energy and RMSD of the heavy atoms compared with the starting coordinates during the 1 ns of molecular dynamics. It is important to monitor the total enery and the RMSD variations in order to determine whether and when the equilibration is reached. As seen from Fig. 4(a,b), the total energy and RMSD remain constant after 800 ps time, indicating that the 3D model of hPKD1c is stable and can be used for subsequent docking calculation.

Docking study: Recently many different classes of hPKD1 inhibitors have been reported, including Gö6976 **1**[27] and CID75567 **3**[28]. However, the mechanism by which these inhibitions achieve potency and selectivity for hPKD1 remains unknown, due in large party to a death of structural information on enzyme-inhibitor complexes. Furthermore, an intriguing aspect of hPKD1 inhibition which has arisen in the literature is that Gö6976 **1** and its analogues were high specificity and

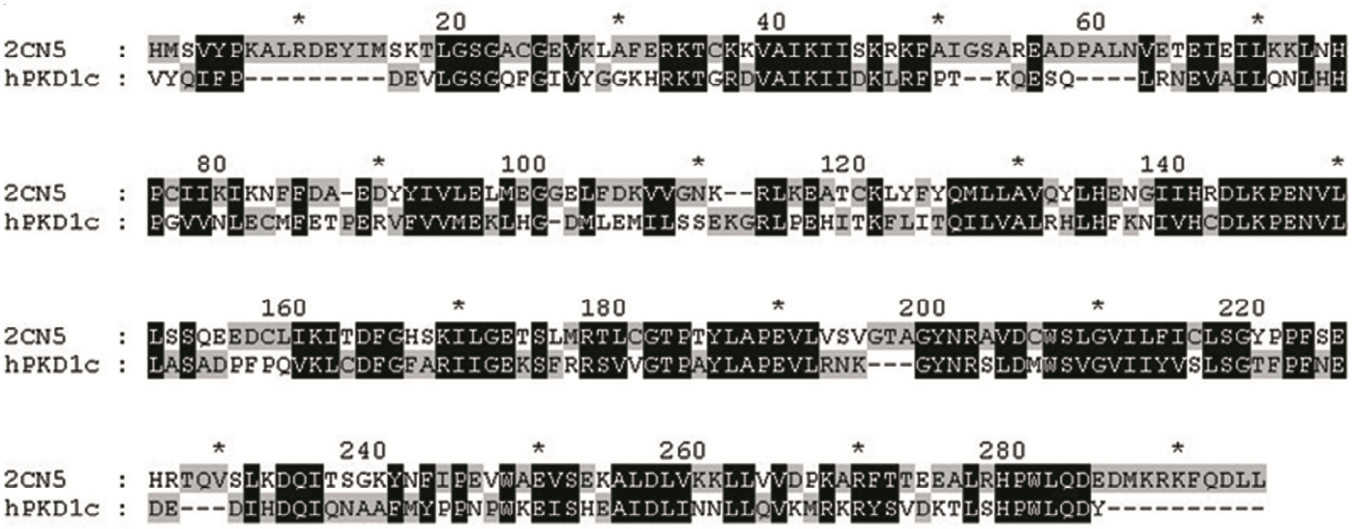

Fig. 2. Sequence alignment of hPKD1 and 2CN5

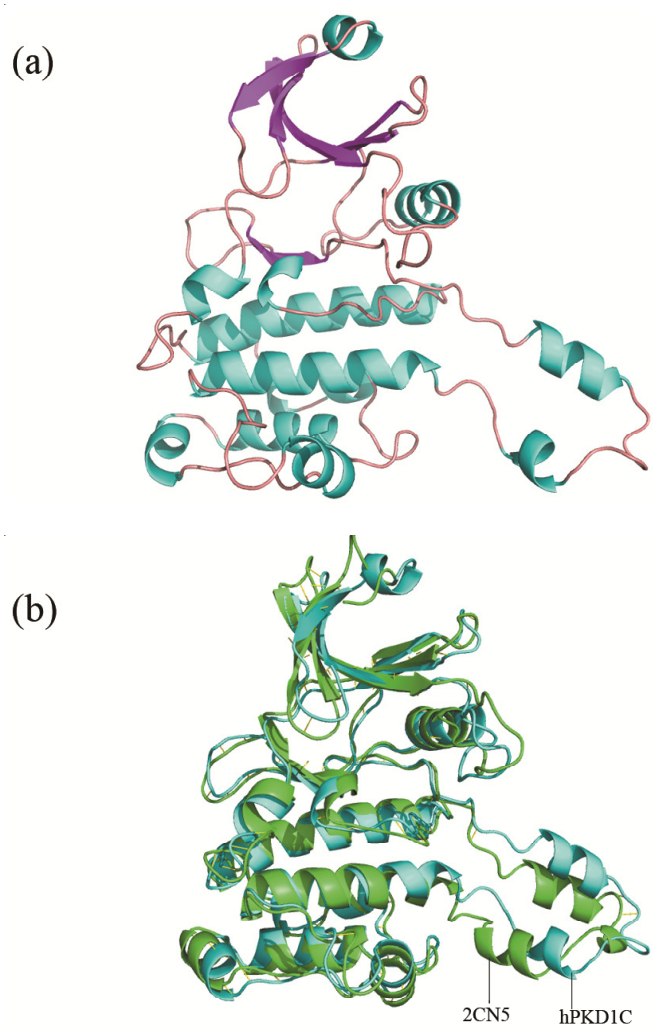

Fig. 3. (a) The final 3D-structure of hPKD1 (b) Comparison of the refined hPKD1 model with its template 2CN5. The blue ribbon is a representation of the hPKD1. The green ribbon is a representation of 2CN5

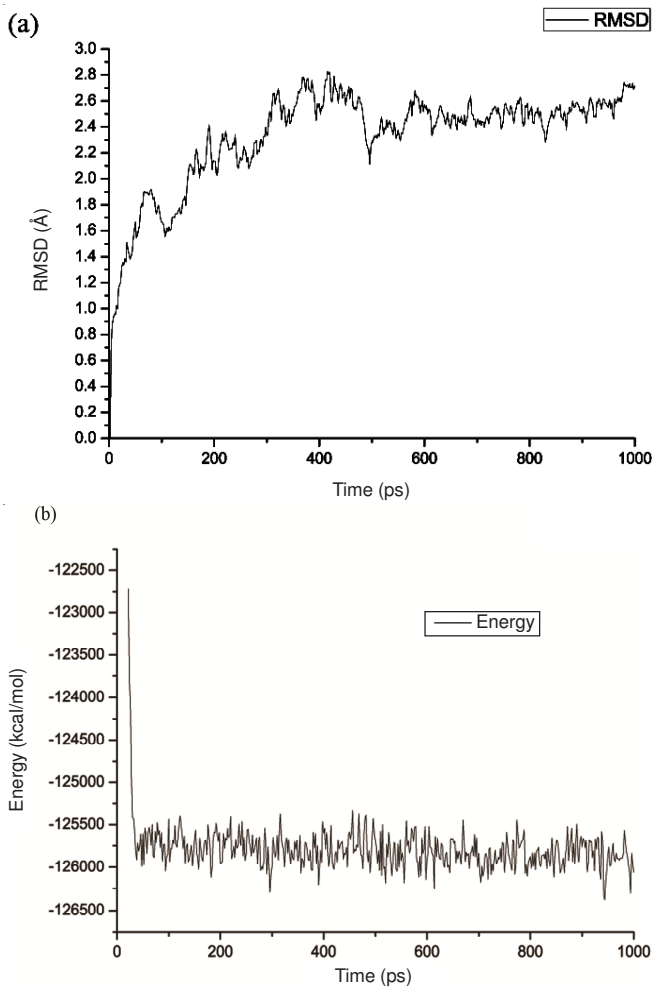

Fig. 4. (a) RMSD with respect to simulation time for a 1ns free MD simulation on the hPKD1 and (b) the total energy

potent inhibition of hPKD1 *in vitro*. In the following discussion, the interactions of the ligands with the receptor in the modeled complexes are investigated and we shall compare the inhibition ability of hPKD1c by Gö6976 **1** with that by its structural analogues. These complexes will reveal how inhibitors achieve potency and specificity for hPKD1, thus offering key insights into guide future drug design efforts.

Docking module and the binding 3D conformation of the complex is described in Fig. 5(a). In order to determine the

key residues that comprise the active site of the model, the interaction energies of the substrate with each of the residues in the active site were calculated. Significant binding-site residues in the models were identified by the total interaction energy between the ligand and each amino acid residues in the enzyme. This identification, compared with a definition based on the distance from the substrates, can clearly show the relative significance for every residue. Table-1 gives the interaction energies including the total, van der Waals and electrostatic energies with total energies lower than -1.0 kcal mol^{-1}.

As seen from the Table-1 the enzyme-substrate complex has a large favourable total electrostatic interaction energy and the total interaction energy is -71.80 kcal mol^{-1}, the van der Waals and electrostatic energies are -18.37 kcal mol^{-1} and -53.43 kcal mol^{-1}, respectively. These results indicate that the attractive interaction is important. Through the interaction analysis, we can know that Ser12, Phe15, Val18, Lys82, Leu83, HIis84, Asp86 and Glu89 are important anchoring residues for Gö6976 **1** and have main contribution to the substrate interaction. For the most residues of the active site such as Ser12, Val18, Lys82, Asp86, Glu89, the interactions energies between hPKD1c and Gö6976 **1** are mainly contributed by electrostatic interactions, while Leu83, Phe15 and His84 are the three amino acid residues that contribute the largest van der Waals interaction energies.

Erik *et al.* reported the structural analogues of Gö6976 **1** are the potential and selective hPKD1 inhibitors. The binding model of 2,6-naphthyridine **13c** with hPKD1c was shown in Fig. 5(b). To determine the key residues that comprise the active site of the model, the interaction energies of the substrate with each of the residues in the active site were calculated. Table-2 gives the interaction energies including the total, van der Waals and electrostatic energies with total energies lower than -1.0 kcal mol^{-1}.

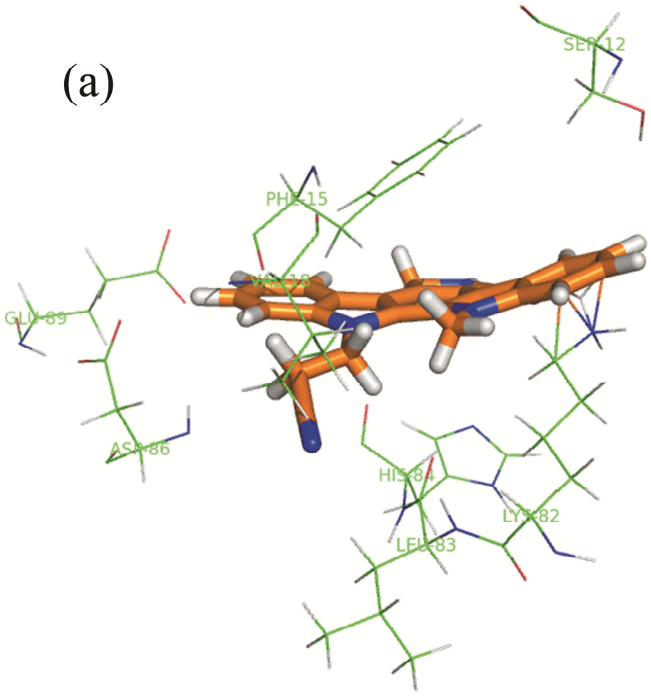

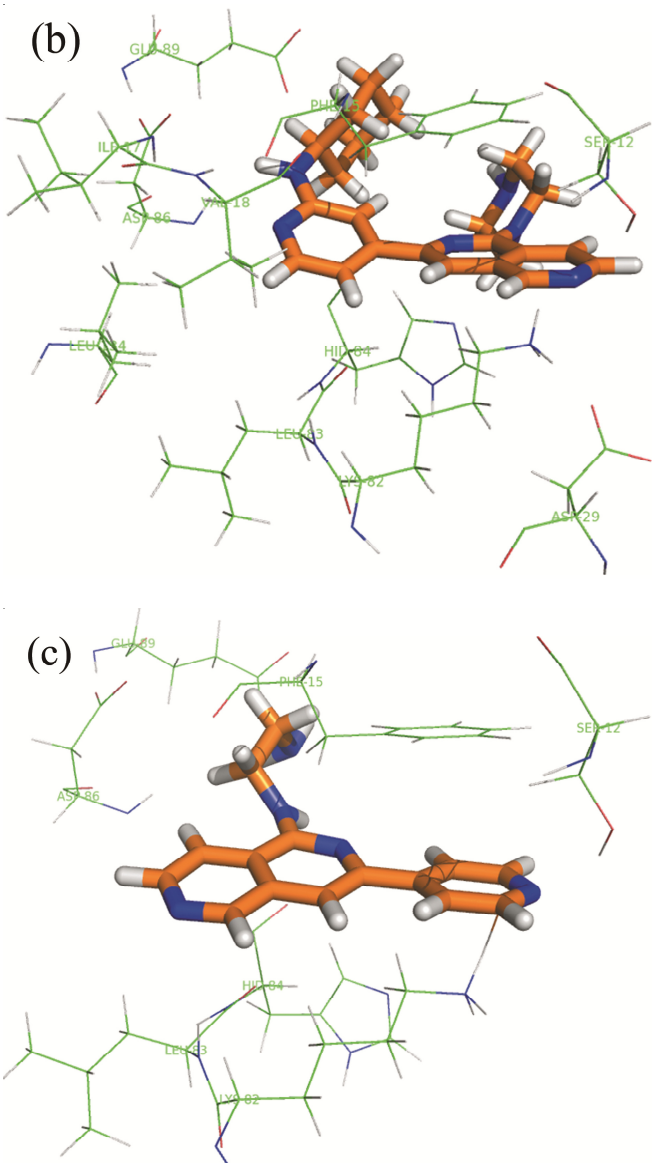

Fig. 5. A close view of the binding of hPKD1 with (a) Gö6976 **1** (b) 2,6-naphthyridine **13c** (c) 2,6-naphthyridine **2**. The ligands and residues are represented by sticks and lines, respectively

TABLE-1
TOTAL ENERGY (E_{total}), VAN DER WAALS ENERGY (E_{vdw}) AND ELECTROSTATIC ENERGY (E_{ele}) BETWEEN INDIVIDUAL RESIDUES OF hPKD1c AND Gö6976 **1** (kcal mol^{-1})

Key residue	Gö6976 **1**		
	E_{total}	E_{vdw}	E_{ele}
SER 12	-4.57	-0.76	-3.81
PHE 15	-4.51	-4.16	-0.34
VAL 18	-7.14	-1.69	-5.45
LYS 82	-19.05	-2.14	-16.92
LEU 83	-2.27	-1.58	-0.69
HIS 84	-5.81	-4.54	-1.26
ASP 86	-11.60	-3.02	-8.58
GLU 89	-16.84	-0.48	-16.36
Total energy	-71.80	-18.37	-53.43

The interaction energy between hPKD1c and 2,6-naphthyridine **13c** was -82.87 kcal mol^{-1}, which has a dramatically increase when compared to the Gö6976-hPKD1c complex. Except for some important residues of the active site such as

TABLE-2
TOTAL ENERGY (E_{total}), VAN DER WAALS ENERGY (E_{vdw}) AND ELECTROSTATIC ENERGY (E_{ele}) BETWEEN INDIVIDUAL RESIDUES OF hPKD1c AND 2,6-NAPHTHYRIDINE **13c** (kcal mol^{-1})

Key residue	2,6-Naphthyridine **13c**		
	E_{total}	E_{vdw}	E_{ele}
SER 12	-7.81	-0.82	-6.99
PHE 15	-6.91	-8.40	1.49
ILE 17	-10.74	-0.40	-10.34
VAL 18	-1.77	-1.31	-0.46
ASP 29	-11.73	-0.55	-11.18
LYS 82	-15.82	-1.77	-14.06
LEU 83	-3.82	-1.48	-2.34
HID 84	-6.28	-4.29	-1.99
ASP 86	-3.81	-3.01	-0.80

Ser12, Phe15, Val18, Lys82, Leu83, HIis84, Asp86 and Glu89, another three important residues Ile17, Asp29 and Leu134 have a large contribution to the high interaction between hPKD1c and 2,6-naphthyridine **13c**.

The 3D conformation of the 2,6-naphthyridine 2 bound with hPKD1c is shown in Fig. 5(c). The interaction energies of 2,6-naphthyridine 2 with hPKD1c dramatically decrease due to the loss of the interactions between some important residues and hPKD1c, such as Asp29 and Leu134. The interaction energy between the inhibitor and the important residues of hPKD1c is listed in Table-3.

TABLE-3
TOTAL ENERGY (E_{total}), VAN DER WAALS ENERGY (E_{vdw}) AND ELECTROSTATIC ENERGY (E_{ele}) BETWEEN INDIVIDUAL RESIDUES OF hPKD1c AND 2,6-NAPHTHYRIDINE **2** (kcal mol^{-1})

Key residue	2,6-Naphthyridine **2**		
	E_{total}	E_{vdw}	E_{ele}
SER 12	-4.47	-0.54	-3.93
PHE 15	-2.69	-3.63	0.93
LYS 82	-17.14	-3.84	-13.29
LEU 83	-2.43	-0.67	-1.76
HIS 84	-1.98	0.78	-2.76
ASP 86	-18.09	-1.59	-16.50
GLU 89	-21.76	-0.87	-20.89
Total Energy	-68.56	-10.36	-58.20

In summary, the analysis of interactions between all three ligands and hPKD1c reveals the fact that electrostatic interaction energy has a larger contribution to ligand binding than VDW interaction energy. Furthermore, there are many common and important residues in the hPKD1c binding to Gö6976 **1**, 2,6-naphthyridine **2** and 2,6-naphthyridine **13c**. Among these ligands, the total energy between hPKD1c and 2,6-naphthyridine **13c** is the highest, whereas the total energy between hPKD1c and 2,6-naphthyridine **2** is the lowest. Compared with 2,6-naphthyridine **2** and 2,6-naphthyridine **13c**, they have the same main moiety, but the only difference is that there exist 2-pyridyl and 4-alkyl moieties in 2,6-naphthyridine **13c**. They both can have strong electrostatic interactions with hPKD1c, whereas the large pyridyl and alkyl moieties in 2,6-naphthyridine **13c** are strong attractive groups and can induce the conformational changes in the active site residues of hPKD1c and make the binding of 2,6-naphthyridine **13c** with hPKD1c more energy favourable. In the case of 2,6-naphthyridine **2**, it essentially has poor interactions with hPKD1c, mainly because it lacks 2-pyridyl and 4-alkyl moieties at two positions of 2,6-naphthyridine and loosely binds to the enzyme, not well fixed in the substrate-binding pocket of the active site. Thus, this explains why the complex of 2,6-naphthyridine **2** and hPKD1c has a lower interaction. The results are in good agreement with the experiment reported by Erik *et al.*[5].

Conclusion

The 3D structure of hPKD1c had not been known. In this investigation, the 3D structure of hPKD1c was built by the homology modeling that was based on the known crystal structure of protein kinase Chk2 (PDB code 2CN5) in complex with ADP. Moreover, energy minimization and molecular dynamics simulation were used to refine the structure. With this model, a flexible docking study was performed and the docking results indicate that the presence and size of substitutions at positions 2 and 6 are critical determinants of potency. Ser12, Phe15, Val18, Lys82, Leu83, HIis84, Asp86 and Glu89 may be the key amino acid residues interacting with the ligands and Ile17, Asp29 and Leu134 may help 2,6-naphthyridine **13c** interact with hPKD1c steadily. These results will offer further experimental studies of structure-function relationships.

ACKNOWLEDGEMENTS

This work is supported by the Dr. Startup Fund of Liaoning Province (20101111) and the Foundation of State Key Laboratory of Theoretical and Computational Chemistry. The authors thank Dr. David A. Case for providing the free software packages.

REFERENCES

1. A.M. Valverde, J. Sinnett-Smith, J.V. Lint and E. Rozengurt, *Proc. Natl. Acad. Sci. U.S.A.*, **91**, 8572 (1994).
2. E. Rozengurt, O. Rey and R.T. Waldron, *J. Biol. Chem.*, **280**, 13205 (2005).
3. Q.J. Wang, *Trends. Pharmacol. Sci.*, **27**, 317 (2006).
4. E.L. Meredith, K. Beattie, R. Burgis and M.J. Capparelli, *J. Med. Chem.*, **53**, 5422 (2010).
5. E.L. Meredith, O. Ardayfio, K. Beattie and M.R. Dobler, *J. Med. Chem.*, **53**, 5400 (2010).
6. S.N. Arun, D. Xie, M.E. Dodd and X.F. Zhong, *J. Dermatol. Sci.*, **60**, 29 (2010).
7. E.R. Sharlow, K.V. Giridhar, C.R. LaValle, J. Chen, S. Leimgruber, R. Barrett, K. Bravo-Altamirano, P. Wipf, J.S. Lazo and Q.J. Wang, *J. Biol. Chem.*, **283**, 33516 (2008).
8. S. Guha, S. Tanasanvimon, J. Sinnett-Smith and E. Rozengurt, *Biochem. Pharmacol.*, **80**, 1946 (2010).
9. C.R. LaValle, K.M. George, E.R. Sharlow and J.S. Lazo, *Biochim. Biophys. Acta*, **1806**, 183 (2010).
10. Q.C. Zheng and C.C. Sun, *J. Theor. Comput. Chem.*, **6**, 141 (2007).
11. F. Pietra, *J. Theor. Comput. Chem.*, **8**, 957 (2009).
12. F. Pietra, *J. Theor. Comput. Chem.*, **9**, 365 (2010).
13. A. Bairoch and R. Apweiler, *Nucl. Acids Res.*, **25**, 31 (1997).
14. S.F. Altschul, T.L. Madden, A.A. Schfer, J.Z. Zhang, W. Miller and D.J. Lipman, *Nucl. Acids Res.*, **25**, 3389 (1997).
15. A. Sali and J.P. Overington, *Protein Sci.*, **3**, 1582 (1994).
16. A. Sali and T.L. Blundell, *J. Mol. Biol.*, **234**, 779 (1993).
17. A. Sali, L. Potterton, F. Yuan, H. Vlijmen and M. Karplus, *Proteins*, **23**, 318 (1995).
18. A. Sali, *Curr. Opin. Biotechnol.*, **6**, 437 (1995).

19. D.A. Case, T.E. Cheatham, T. Darden, H. Gohlke, R. Luo, K.M. Merz, A. Onufriew, C. Simmerling, B. Wang and R.J. Woods, *J. Comput. Chem.*, **26**, 1668 (2005).
20. W.L. Jorgensen, J. Chandraskhar, J. Madura and M.L. Klein, *J. Chem. Phys.*, **79**, 926 (1983).
21. J.P. Rychaert, G. Ciccotti and H.J.C. Berendsen, *J. Comput. Phys.*, **23**, 327 (1977).
22. Y. Duan, C. Wu, S. Chowdhury, M.C. Lee, G.M. Xiong, W. Zhang, R. Yang, P. Cieplak, R. Luo, T. Lee, J. Caldwell, J.M. Wang and P. Kollman, *J. Comput. Chem.*, **24**, 1999 (2003).
23. InsightII Profile-3D User Guide, San Diego: Biosym/MSI (2000).
24. R.A. Laskowski, M.W. MacArthur, D.S. Moss and J.M. Thornton, *J. Appl. Cryst.*, **26**, 283 (1993).
25. M.J. Sippl, *Proteins*, **17**, 355 (1993).
26. Discovery Studio, Version 2.5. San Diego.
27. M. Gschwendt, S. Dieterich, J. Rennecke and W. Kittstein, *FEBS Lett.*, **392**, 77 (1996).
28. E.R. Sharlow, K.V. Giridhar, C.R. Lavalle and J. Chen, *J. Biol. Chem.*, **283**, 33516 (2008).